Organs-on-a-Chip 3 (2021) 100011

Contents lists available at ScienceDirect

Organs-on-a-Chip

journal homepage: www.sciencedirect.com/journal/organs-on-a-chip

Isolation and characterisation of graves' disease-specific extracellular vesicles from tissue maintained on a bespoke microfluidic device

Hayley Foster [a], Mark Wade [a], James England [b], John Greenman [a], Victoria Green [a,*]

[a] University of Hull, Faculty of Health Sciences, Hull, HU6 7RX, UK
[b] Hull and East Yorkshire Hospitals NHS Trust, Department of Otorhinolaryngology, Head and Neck Surgery, Hull, HU16 5JQ, UK

ARTICLE INFO

Keywords:
Graves' disease
Microfluidics
Extracellular vesicles
Exosomes

ABSTRACT

This report demonstrates the ability of a microfluidic device to maintain human Graves' disease tissue enabling the isolation and characterisation of Graves' disease specific exosomes. Graves' disease (n = 7) and non-Graves' disease (Hashimoto's thyroiditis, n = 3; follicular adenoma, n = 1) human tissue was incubated in a microfluidic device for 6 days ± dexamethasone or methimazole and effluent was analysed for the size and concentration of extracellular vesicles (EV) using nanoparticle tracking analysis. Exosomes were isolated by centrifugation and characterised using Western blotting and qRT-PCR for miRNA-146a and miRNA-155, previously reported to be immunomodulatory. EV were detected in all effluent samples. No difference in concentration was observed in the EV released from Graves' compared to non-Graves' disease tissue and although the size of EV from Graves' disease tissue was smaller compared to those from non-Graves' disease tissue, the difference was not consistently significant. No effect of treatment was observed on the size or concentration of EV released. The exosome markers CD63 and CD81 were detectable in 2/5 Graves' disease tissue exosomes and CD63 was also evident in exosomes from a single non-Graves' sample. miRNA-146a and miRNA-155 were detectable in all samples with no difference between tissue cohorts. Treatment did not influence miRNA expression in exosomes isolated from Graves' disease tissue. Although miRNA-146a and miRNA-155 were both elevated following treatment of non-Graves' disease tissue with dexamethasone and methimazole, the increase was not significant. This study provides a proof of concept that incubation of tissue on a microfluidic device allows the detection, isolation and characterisation of extracellular vesicles from human tissue biopsies.

1. Introduction

Graves' disease is an autoimmune disease affecting 3% of women and 0.5% of men (Antonelli et al., 2020). It is characterised by elevated circulating autoantibodies to the thyrotropin receptor (TRAB), these autoantibodies bind to the thyrotropin receptor (TSHR) on thyroid follicular epithelial cells stimulating thyroid growth and hormone synthesis/secretion via cyclic adenosine monophosphate (cAMP) production resulting in hyperthyroidism (Edo et al., 2019). Inflammation, characteristic of Graves' disease can lead to thyroid associated orbitopathy/ophthalmopathy, an eye disease, which occurs in 30–50% of Graves' disease patients, with 5% leading to blindness (Tanda et al., 2013). Despite extensive research, the pathogenesis of this disease remains unclear.

Exosomes and microvesicles (collectively known as extracellular vesicles; EV) are membrane bound vesicles, released from all cells (Zhang et al., 2020; Fig. 1). They are found in all biological fluids, have a molecular profile representative of the cellular source and microvesicles are elevated in the blood of patients with Graves' disease (Mobarrez et al., 2016). EV are thought to be key players in intercellular communication both locally and systemically and have been shown to activate the immune system and trigger inflammation in many disease states (Jiang et al., 2020; Yang and Liu, 2020; Lanyu and Feilong, 2019), either by direct stimulation of $CD4^+$ T cells or via phagocytosis and presentation by dendritic cells (Mittal et al., 2020). In addition, EV are able to inhibit the apoptosis of activated T cells exacerbating the inflammatory response, as shown in patients with rheumatoid arthritis whose EV, which have higher levels of membrane bound tumour necrosis factor-α compared with those from healthy controls, could prevent apoptosis in activated T cells (Zhang et al., 2006).

* Corresponding author. Daisy Research Laboratories (2nd Floor), Castle Hill Hospital, Hull, HU16 5JQ, UK.
E-mail addresses: H.Foster-2018@hull.ac.uk (H. Foster), M.Wade@hull.ac.uk (M. Wade), James.England@hey.nhs.uk (J. England), j.greenman@hull.ac.uk (J. Greenman), v.l.green@hull.ac.uk (V. Green).

https://doi.org/10.1016/j.ooc.2021.100011
Received 6 June 2021; Received in revised form 8 November 2021; Accepted 12 November 2021
Available online 17 November 2021

The main first line treatment for Graves' disease involves the use of thionamides such as carbimazole or the metabolite methimazole, which reduce inflammation and thyroxine production (Kahaly, 2020). However, this class of drugs does not specifically target the underlying pathogenic process and when used for definitive management, relapse rates are high after withdrawal (40–60%; Liu et al., 2015). Other treatment options include radioiodine and/or surgical ablation both of which destroy/remove thyroid tissue resulting in high rates of hypothyroidism (90–100%). Additional treatment with the anti-inflammatory corticosteroid, dexamethasone has been trialled (Mao et al., 2009), with the aim of down regulating the inflammatory response. The results of this trial showed a reduction in serum TRAB, thyroid volume and relapse rate following treatment (Mao et al., 2009). Patients with active, moderate/severe Graves' ophthalmopathy are commonly treated with dexamethasone (Bartalena et al., 2016; Längericht et al., 2020), but the use of dexamethasone as a treatment for Graves' disease *per se* remains controversial due to side effects including acute/severe liver damage (Mao et al., 2009).

It is postulated that EV and specifically small EV/exosomes (sEV); containing specific microRNAs (miRNAs) released from Graves' tissue may stimulate the inflammatory immune response, aggravating the disease further and contributing to Graves' ophthalmopathy, as increased miRNA-155 (a single stranded, small, non-coding RNA) has the potential to promote ocular inflammation and proliferation in this disease (Ma et al., 2011; Li et al., 2014). MiRNA are small (17–25 nucleotides) non-coding RNA, whose primary role is gene regulation (Catalanotto et al., 2016). If carbimazole and dexamethasone reduce the release of exosomes, therapies alternative to dexamethasone with its associated side effects, which target EV and/or their contents directly, can be developed.

The majority of EV work to date has been carried out on either cell lines or serum/plasma. Although serum and plasma are a rich source of EV, they contain a mix of vesicles derived from various cell types of both healthy and diseased origin, making characterisation complicated. In contrast, those derived from cell lines are from a single cell source, which may not be representative of the multicellular nature of the tissue. The use of microfluidics to culture small ($3mm^3$) pieces of human tissue (Bower et al., 2017; Cheah et al., 2017), provides the distinct advantage of being able to isolate EV known to originate from the diseased thyroid and associated cells.

Although many researchers have reported the culture of a diverse range of human tissue explants/slices *ex vivo* under static conditions (Contartese et al., 2020), the clinical relevance of these models is uncertain. Microfluidic systems have advanced *ex vivo* culture by providing a controlled fluid flow for nutrient exchange, removal of waste and also induce shear stress, aiming to recapitulate the *in vivo* microenvironment. Whilst many groups have successfully developed microfluidic devices to maintain engineered tissues/organoids, including brain, liver, heart, intestine, lung, skin and kidney (reviewed in Yu et al., 2019 and Duzagac et al., 2021), patient biopsies possess the whole gamut of cells and extracellular matrix present in the parent tissue which provides a closer representation of the disease. Recently, dynamic perfusion systems, including microfluidic based chips, have demonstrated the ability to maintain human organotypic cultures from tissues including heart, liver, ovary, breast, rectum and larynx (Hughes et al., 2021). The 3D complexity of the tissue is retained and mimics the *in vivo* environment, resulting in a significant advantage over *in vitro* 2D culture of artificially immortalised cell lines, which lack critical cellular interactions when studied in isolation. *Ex vivo* microfluidic models, span the gap between high throughput use of cell lines and complex, expensive *in vivo* models (McLean et al., 2018).

The authors have developed and characterised several microfluidic devices for the successful maintenance of a variety of human tissues (cardiac tissue, and tumour biopsies from colorectal, thyroid and head and neck squamous cell carcinomas, HNSCC; Bower et al., 2017; Cheah et al., 2010, 2017; Hattersley et al., 2011; Carr et al., 2014; Dawson et al., 2016; Kennedy et al., 2019; Riley et al., 2019). The aim of the current study was to determine whether EV can be isolated and characterised from effluent coming from the microfluidic devices containing Graves' disease and non-Graves' disease tissue. The effect of treatment with the clinically relevant drugs, dexamethasone and methimazole on EV release, size and miRNA content has also been investigated.

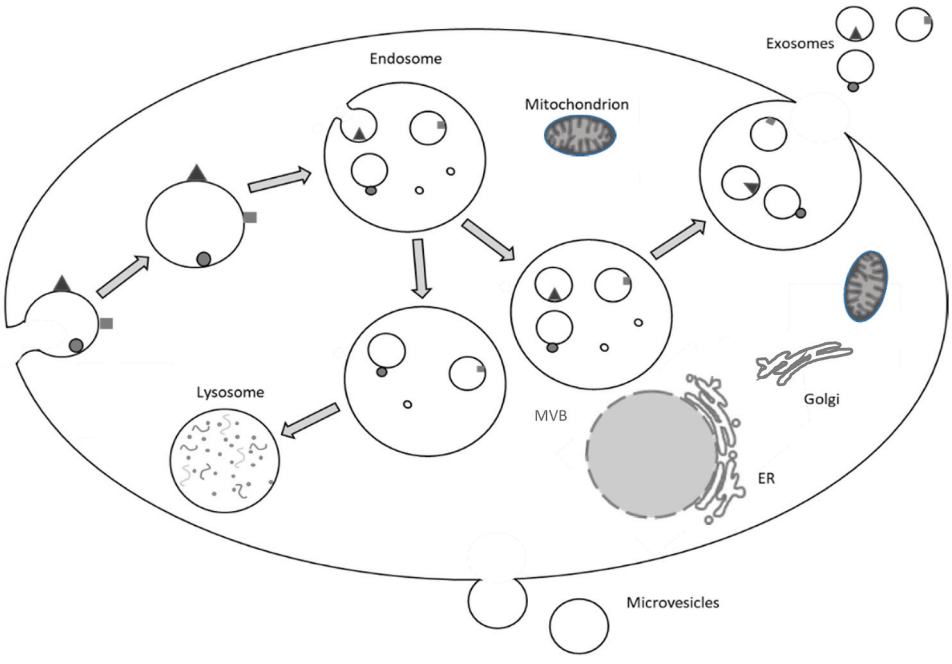

Fig. 1. Schematic demonstrating exosome formation and release. Unlike microvesicles which are formed from the direct outward budding of the cell membrane, exosomes or sEV are formed from the inward budding of the endosomal membrane to form multivesicular bodies (MVB). The MVB either fuse with lysosomes and their content is enzymatically degraded, or they fuse with the cell membrane to release their contents as exosomes (adapted using (Zhang et al., 2020).

2. Materials and methods

Ethical approval for the study was obtained from London Hamstead Research Ethics committee (17/LO/0209) and from Hull University Teaching Hospitals NHS Trust research and development (R2469). Tissue samples were obtained from either patients with Graves' disease (n = 7) or from patients with non-Graves' related thyroid pathologies (n = 4; Hashimoto's or follicular adenoma) undergoing total thyroidectomy following written informed consent (Table 1), from the ENT department at Castle Hill Hospital, Hull.

2.1. Setting up and running microfluidic devices

The microfluidic device was designed and manufactured in Hull out of Perspex (Fig. 2). The chip comprises a central, 4mm diameter chamber, to house the tissue, which is flanked by two Perspex screw in connectors, each containing 13 holes of 0.1mm diameter, connected via ethylene tetrafluoroethylene (ETFE) 1/16" tubing (Kinesis Ltd, St Neots, UK). The inlet tubing is connected to a 20ml syringe (Becton Dickinson, Wokingham, UK) via a 0.2μm filter (Sarstedt Ltd, Leicester, UK) and a one-piece leak free connector (Mengel Engineering, Denmark).

On receipt of the tissue biopsy, the sample was divided using scalpels into pieces (~15mg each) before being placed into six separate microfluidic devices, within 1hr of receipt, and perfused (2μl/min) using a calibrated pressure driven pump (PhD Harvard, 2000), with Dulbecco's modified eagles medium (DMEM) containing 10% (v/v) exosome depleted foetal bovine serum (Gibco, Fisher Scientific), penicillin/streptomycin (0.1U/ml and 0.1mg/ml respectively; Lonza, Castleford, UK) and L-glutamine (0.4mM; Lonza) alone or including final, physiologically relevant, concentrations of either methimazole (1μg/ml, Sigma) or dexamethasone (0.1μM, Sigma) in duplicate. The microfluidic devices were incubated at 37 °C and perfused continually for 6 days with daily effluent collection. Lactate dehydrogenase (LDH) was analysed using the cytotoxicity detection assay, following the manufacturers' instructions (Merck, Feltham, UK), on effluent released from Graves' (n = 4) and Non-Graves' (n = 3) tissue throughout maintenance on the microfluidic device. Following the assay the absorbance was measured at 492 nm and normalised/mg of starting tissue. Lysis of the tissue was achieved with 10% lysis solution (provided in the kit). Remaining effluent was stored at −80 °C prior to analysis and EV isolation, with each sample undergoing a single freeze thaw cycle. Hematoxylin and eosin staining of paraffin embedded tissue sections prior to and post microfluidic maintenance was performed as previously described (Riley et al., 2019).

2.2. Nanoparticle tracking analysis (NTA)

The effluents collected from all samples, following perfusion on the microfluidic device, were analysed for EV size and concentration using the Malvern Panalytical® NanoSight LM10. For each sample, three runs of 60 s were used to analyse the EV. The mean concentration of the particles was normalised/10mg of starting tissue for comparison between samples.

Table 1
Patient clinicopathological characteristics.

Sample No	Graves' or non Graves'	Sex	Age	NTA	WB	qRTPCR
GRA11	Graves'	F	61	✓	–	✓
GRA12	Graves'	F	44	✓	✓	✓
GRA13	Graves'	M	47	✓	✓	✓
GRA14	Graves'	F	62	✓	✓	✓
GRA15	Graves'	F	53	✓	✓	✓
GRA16	Follicular adenoma	F	39	✓	–	✓
GRA17	Graves'	F	23	✓	–	✓
GRA18	Hashimoto's	F	66	✓	✓	–
GRA19	Graves'	F	36	✓	✓	–
GRA20	Hashimoto's	F	29	✓	–	✓
GRA21	Hashimoto's	F	75	✓	–	✓

NTA, nanoparticle tracking analysis; WB, Western blotting; qRTPCR, quantitative reverse transcriptase polymerase chain reaction.

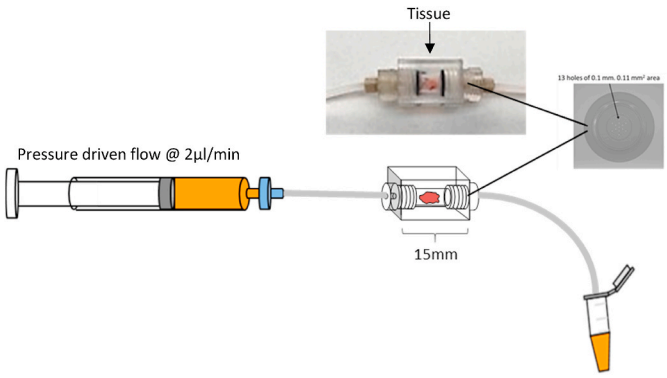

Fig. 2. Schematic of a continuous flow microfluidic device. A rectangular device (15 x 10 × 10 mm) has been CNC milled out of PMMA (Perspex). The inner core is a cylinder 4mm in diameter which houses the tissue. On each side, tubing (ethylene-tetrafluoroethylene, 0.8mm internal diameter) is connected via a port with 13 holes of 0.1 mm diameter to create an even flow (2μl/min) of fluid across the tissue. The chamber is sealed with two O-rings (4 mm inner diameter, 1 mm thickness).

2.3. Ultracentrifugation to isolate small extracellular vesicles (exosomes)

EV were isolated from the tissue effluent coming from the microfluidic device using sequential centrifugation steps as described by Théry et al. (2006).

Briefly, the conditioned medium from duplicate devices were combined from days 4, 5 and 6 of perfusion and centrifuged at 400 x *g* for 10 min at 4 °C. The supernatant was transferred to a new falcon tube and sequentially centrifuged at 2, 000 x *g* (10 min), and 10, 000 x *g* at 4 °C (30 min; Beckman Coulter Ltd, High Wycombe, UK). Supernatants were transferred into OptiSeal tubes (Beckman Coulter) for ultracentrifugation in a TLA-110 fixed angle rotor at 100, 000 x *g* at 4 °C for 1 h (Beckman Optima MAX-XP). The sEV pellet was washed with PBS and ultracentrifuged again for 1h. The supernatant was removed and the tube inverted for 10 min prior to protein or RNA extraction.

2.4. Western blot analysis of exosomal content

Protein was extracted from sEV pellets (in the effluent from 5 Graves' patient samples and one non-Graves' tissue sample maintained on the microfluidic devices) using 20μl RIPA buffer containing PhosSTOP – phosphatase inhibitor cocktail and protease inhibitor cocktail complete ULTRA (Sigma). Lysates from replicate tubes were combined and incubated for 15 min on ice before vortexing and sonication for 3 min to fully disrupt the sEV. Centrifugation at 4 °C for 15 min at 16,000 x *g* pelleted cell debris and the supernatant was analysed for protein content using the Pierce™ BCA protein assay kit (Thermofisher Scientific).

Western blotting for the exosomal markers CD9, CD63 and CD81 was performed using the non-reducing Bolt system (Thermofisher Scientific) as described by Kowal et al. (2017). Briefly, 30μl of sEV extract was added to 10μl of 4 × Bolt sample buffer (Thermofisher Scientific) and heated to 70 °C for 10 min before loading onto a 4–12% Bis-Tris gel (Thermofisher Scientific) submerged in 1 × MES running buffer. Proteins were separated at 150V until the dye front reached the bottom of the gel before being transferred onto PVDF membranes (BioRad) using the BioRad Turbo Transblot semi-dry transfer system.

PVDF membranes were blocked in 5% (w/v) milk powder in TBS-Tween-20 (0.1% v/v) for 1hr before being probed with primary antibodies for CD9 (C-4; 1:250–1:2000), CD63 (MX-49.129.5; 1:500–1:2000), CD81 (0.N.165; 1:250–1:500; Santa Cruz/Insight

Biotechnology, Middlesex, UK) for either 1hr at room temperature or overnight at 4 °C. Following 3 × 10min washes with TBS-Tween (0.1%), primary antibodies were detected using mouse-IgG Kappa binding protein-HRP (1:5000; Insight Biotechnology) for 1hr before further washes and chemiluminescent detection (SuperSignal™ West Pico PLUS Chemiluminescent Substrate; Thermofisher Scientific) and X-ray autoradiography.

2.5. RNA extraction and qRT-PCR

RNA was extracted from each sEV pellet following ultracentrifugation (sEV collected from 6 Graves' tissues and 3 non-Graves' tissues) using the miRNeasy micro kit (Qiagen, Manchester, UK), following the manufacturer's instructions. Briefly, 700μl of Qiazol reagent (Qiagen, Manchester, UK) was added to each sEV pellet followed by 140μl chloroform. Following incubation for 2–3min the suspension was centrifuged at 12, 000 x *g* at 4 °C for 15 min to separate the phases. The upper aqueous phase was combined with 1.5 vol of 100% ethanol and applied to an RNeasy MiniElute spin column in a 2ml collection tube, before centrifuging at >8000 x *g* for 15s at room temperature. The column was washed with RWT (700μl) and RPE buffers (500μl; supplied) followed by 80% ethanol (500μl) with centrifugation at >8000 between each. The spin column was dried by centrifuging at 16, 000 x *g* for 5 min, before being placed in a new collection tube. RNase free water (14μl) was applied to the column before centrifugation at 16, 000 x *g* for 1 min to elute the RNA. This was stored at −80 °C prior to cDNA synthesis.

cDNA was synthesised using the miRCURY locked nucleic acid (LNA) RT kit (Qiagen), following the manufacturer's instructions using 4μl of prepared RNA. The reaction mix was incubated for 60 min at 42 °C with a 5 min denaturation step at 95 °C.

qRT-PCR was performed using the miRCURY SYBR green PCR kit (Qiagen) with individual miRCURY LNA miRNA PCR assays using manufactured primers for hs-miRNA-146a-5p and hs-miRNA-155–5p (Qiagen). Primers for hs-miRNA-16–5p (Qiagen) were used as an endogenous control (Lee et al., 2015), following trials using the same amount of RNA from both treated and untreated samples and being shown not to alter with treatment. Each PCR reaction mixture was prepared using 2 × miRCURY SYBR green Master mix (5μl), ROX reference dye (0.5μl), LNA primer mix (1μl) and RNAse free water (0.5μl). cDNA (3μl, 1:30 diluted) was added to triplicate wells of an Applied Biosystems™ MicroAmp™ Fast Optical 96-well reaction plate, along with 7μl of reaction mix. Following a brief centrifuge the PCR was completed on an ABI StepOnePlus™ system with the following settings: Initial heat activation 95 °C for 2 min followed by 40 cycles of 95 °C for 10 s and 56 °C for 60 s. Melt curve analysis was performed at 60–95 °C. Relative expression/fold change of miRNA-146a and miRNA-155 relative to miRNA-16 was determined using the comparative cycle threshold (CT) method ($2^{-\Delta\Delta CT}$; Livak and Schmittgen, 2001).

2.6. Statistical analysis

Two-way ANOVA (GraphPad Prism v.9.1.0; 221) with bonferroni correction was used to determine changes in the release of extracellular vesicles over time and with treatment and to compare between Graves' and non-Graves' samples. One-way ANOVA was used with multiple comparisons to compare miRNA expression in exosomes extracted following both treatments to the control using Dunnetts' test. The expression of each miRNA in the sEV was compared between those extracted from Graves' tissue and those extracted from non-Graves' tissue for both dexamethasone treated and methimazole treated samples using Mann Whitney *U* test.

3. Results

3.1. Lactate dehydrogenase release from thyroid tissue maintained on the microfluidic device

A higher level of LDH release was observed at the start of the experiment reflecting the tissue damage during slicing. This decreased to a basal level throughout the remainder of the experiment (representative result shown in Fig. 3). Lysis of the tissue at the end showed an increase in LDH indicating the presence of viable cells.

3.2. The release of extracellular vesicles from graves' and non-graves' tissue maintained on the microfluidic device

NTA was carried out on the effluent collected from all the thyroid tissue samples with and without dexamethasone and methimazole. An initial high level of EV release was observed between 0 and 3 days in both types of tissue (Fig. 4) which significantly decreased over time ($p<0.0001$) before stabilizing throughout days 4–6 (~2.95 x 10^8 particles/ml/10mg tissue). No significant difference in the concentration of particles released was observed between Graves' and non-Graves' tissue. The mean size of particles released, ranged from 138nm to 233nm, with a significant decrease in size observed in both tissue types over time (Fig. 5; $p<0.0001$). At each time point the size of particles released from non-Graves' tissue was greater than those released from Graves' tissue however, the difference was only significant at the 0–4hr time point ($p = 0.0007$; control, $p = 0.0102$; dexamethasone and $p<0.0001$; methimazole).

3.3. The effect of treatment on the release of extracellular vesicles from graves' and non-graves' tissue

The results from individual patients were variable and although both dexamethasone and methimazole appeared to increase particle release over the first three days in non-Graves' tissue, no consistent or significant treatment effects were observed in either tissue cohorts (Fig. 4). Treatment also had no significant effect on the size of the particles released from tissue.

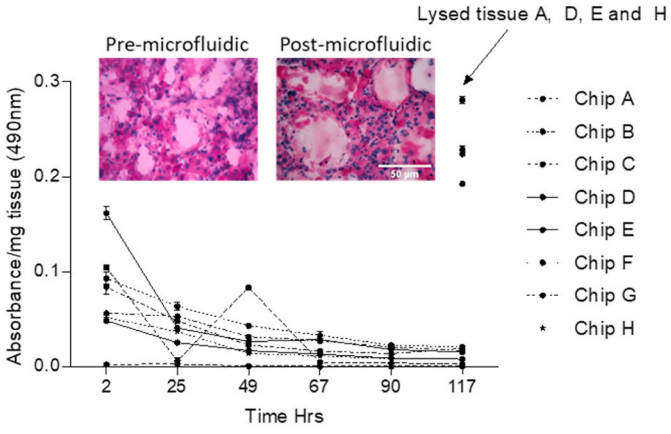

Fig. 3. Lactate dehydrogenase (LDH) release from a representative non-Graves' disease tissue throughout maintenance on-chip. Control, medium only (chip A and B), dexamethasone treated (chip C and D), methimazole treated (chip E and F). LDH release following lysis of tissues from chip A, D, E and H indicated by the arrow. The mean absorbance/mg tissue ± SD from duplicate readings of the effluent is displayed. Insert shows hematoxylin and eosin stained non-Graves' tissue pre and post on-chip maintenance ×400 magnification.

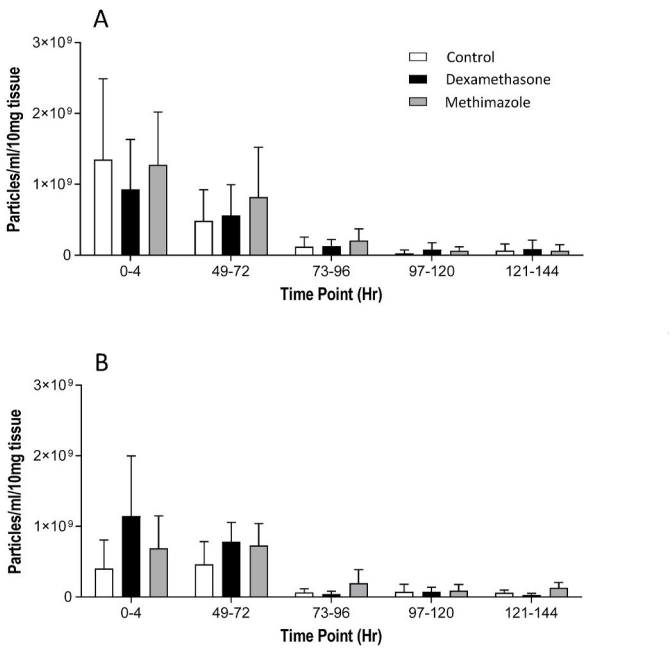

Fig. 4. Nanoparticle tracking analysis of extracellular vesicles (concentration) released from A) Graves' biopsy samples (n = 7) and B) non-Graves' biopsy samples (n = 4), maintained on the microfluidic device over a 6 day period (diluted 1:4 with serum free medium), to investigate the effect of treatment on extracellular vesicle release. The mean concentration of EV released from the 7 Graves' samples and the 4 non-Graves' samples are expressed as particles/ml/10mg starting weight of tissue ± SD. A significant decrease in particle release was observed over time from both tissue types ($p<0.0001$), Two Way ANOVA.

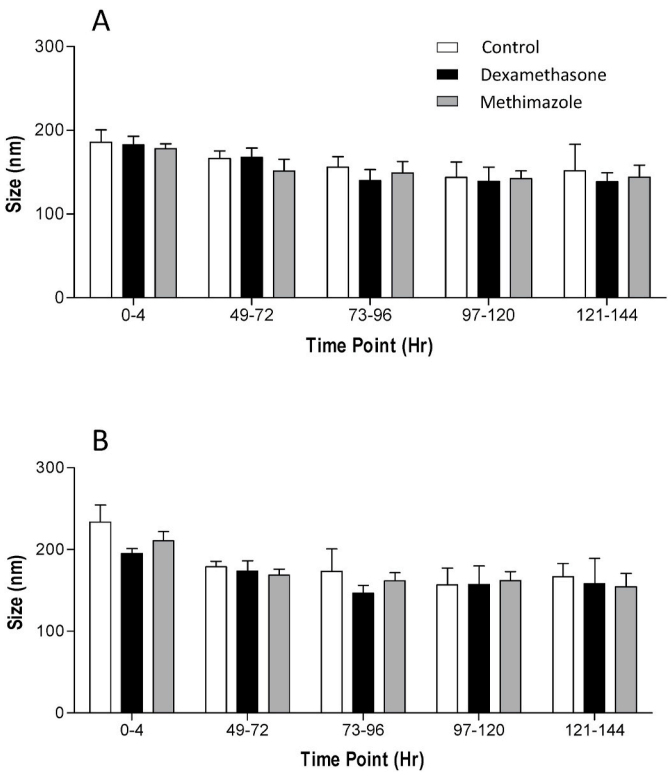

Fig. 5. Nanoparticle tracking analysis of extracellular vesicles (size) released from A) Graves' biopsy samples (n = 7) and B) non-Graves' biopsy samples (n = 4), maintained on the microfluidic device over a 6 day period (diluted 1:4 with serum free medium). The mean size (nm) from the 7 Graves' samples and the 4 non-Graves' samples ± SD is displayed. A significant decrease in particle size was observed over time from both tissue types ($p<0.0001$), Two Way ANOVA.

3.4. Detection of CD9, CD63 and CD81 on EV released from graves' and non-graves' disease tissue

Following combination of the effluents from days 4, 5 and 6, the approximate volume processed from each sample for sEV isolation was 4.5ml. The protein concentration obtained from the subsequent sEV lysates ranged from 48.5 to 231μg/ml, however the maximum volume of 30μl of protein lysate was added to appropriate wells to give the best chance of detection. CD63 was detected in the sEV released from 2/5 Graves' disease tissues and from the single non-Graves' tissue investigated (Fig. 6A), whereas CD81 was only detected in the sEV released from 2 of the Graves' patients (Fig. 6B). CD9 was not detectable in any of the sEV lysates.

3.5. miRNA expression in EV released from Graves' and non-Graves' tissue

The volume of effluent used for sEV isolation and RNA extraction is shown in Table 2. Detectable amounts of RNA, measured using nanodrop, were found in all samples and this ranged from 7.9ng/μl up to 43,7ng/μl. Surprisingly, the amount of RNA extracted was not always proportional to the volume of starting effluent shown by the ratio of RNA concentration/starting volume (Table 2). In the Graves' patients (n = 6), both miRNA-146a and miRNA-155 were detectable in all cases, but there was no significant effect of treatment on the expression as determined using fold change compared to control ($2^{-\Delta\Delta}$CT) with one-way ANOVA (Dunnetts' test; Fig. 7A). In contrast, both miRNA-146a and miRNA-155 appeared to increase in expression in the exosomes released from non-Graves' tissue, following treatment with both dexamethasone and methimazole, with methimazole having a greater effect (Fig. 7B). However, only three non-Graves' samples were used for qRT-PCR and the variation within these patients was substantial, meaning that the differences were not significant. In addition, no significant difference in the expression of either miRNA-146a or miRNA-155 was observed between Graves' disease exosomes and non-Graves' disease exosomes when comparing the fold change for both treatments.

4. Discussion

This report has demonstrated, for the first time, the isolation of tissue-specific sEV from small pieces of human tissue maintained on a microfluidic device. It has shown that these vesicles can be quantified using NTA and the sEV can be retrieved and characterised using molecular techniques. Although the effluent was frozen prior to analysis, which can reduce the numbers of detectable EV, there were still a substantial amount of EV present, observed using NTA, even after a 1:4 dilution, therefore any clear treatment effects should still be observed.

Isolation of EV from tissue has, until now, been limited to the extraction from the interstitial space of, for example; mouse brain and lung tumours, using gentle tissue dissociation followed by ultracentrifugation and sucrose density gradient centrifugation (Hurwitz et al., 2019; Perez-Gonzalez et al., 2017).

The use of dynamic microfluidic tissue perfusion to maintain functional (thyroxine production throughout culture) benign and thyroid tumour tissue, for up to 4 days, has been demonstrated previously by the authors (Riley et al., 2019). Riley and colleagues demonstrated that thyroid tissue viability was unaffected by microfluidic culture using propidium iodide and trypan blue staining of dissociated cells. In agreement with the current study, tissue morphology (H&E) was not affected by maintenance on-chip and LDH release was initially elevated, likely due to tissue manipulation and subsequently decreased to minimal levels over the period of maintenance on-chip. An increase in the LDH release following cell lysis, as demonstrated in both studies, indicates

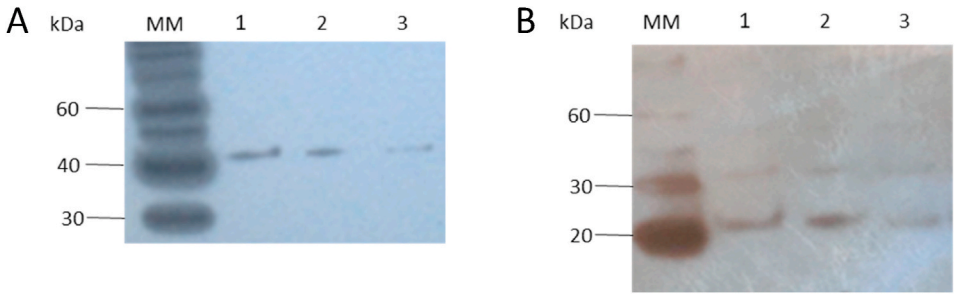

Fig. 6. Western blot analysis of EV released from a representative Graves' disease tissue sample, incubated on a microfluidic device. A) CD63 B) CD81. EV released from; lane 1, control tissue; lane 2, dexamethasone treated tissue; lane 3, methimazole treated tissue. MM – Magic Mark XP western protein standard.

Table 2
RNA concentration of the lysate obtained from EV released from Graves' and non-Graves' tissue maintained on a microfluidic device.

Graves'	Treatment	Volume extracted from (ml)	RNA concentration (ng/μl)	Ratio of RNA concentration/original volume
GRA11	Control	4.7	ND	–
	Dexamethasone	4.7	16.1	3.4
	Methimazole	4.7	8.6	1.8
GRA12	Control	4.7	7.5	1.6
	Dexamethasone	4.7	8.8	1.9
	Methimazole	4.7	8.2	1.7
GRA13	Control	4.7	8.6	1.8
	Dexamethasone	3.7	15.4	4.2
	Methimazole	4.7	12	2.6
GRA14	Control	6	25.2	4.2
	Dexamethasone	6	13.7	2.3
	Methimazole	3.7	10.1	2.7
GRA15	Control	3.0	14	4.7
	Dexamethasone	3.0	13.9	4.6
	Methimazole	4.6	15.3	3.3
GRA17	Control	13.4	39.9	3.0
	Dexamethasone	14.1	35.4	2.5
	Methimazole	9.4	10.9	1.2
Non-Graves'				
GRA16	Control	9.4	43.7	4.7
	Dexamethasone	9.4	39.3	4.2
	Methimazole	9.4	33.3	3.5
GRA20	Control	2.6	9.9	3.8
	Dexamethasone	4.1	7.9	1.9
	Methimazole	4.7	41.2	8.8
GRA21	Control	4.5	10.5	2.4
	Dexamethasone	4.6	25.7	5.6
	Methimazole	4.5	15.9	3.5

ND = Not done.
Note: Volume varied due to the use of effluent for nanosight analysis and western blotting in addition to RNA extraction.

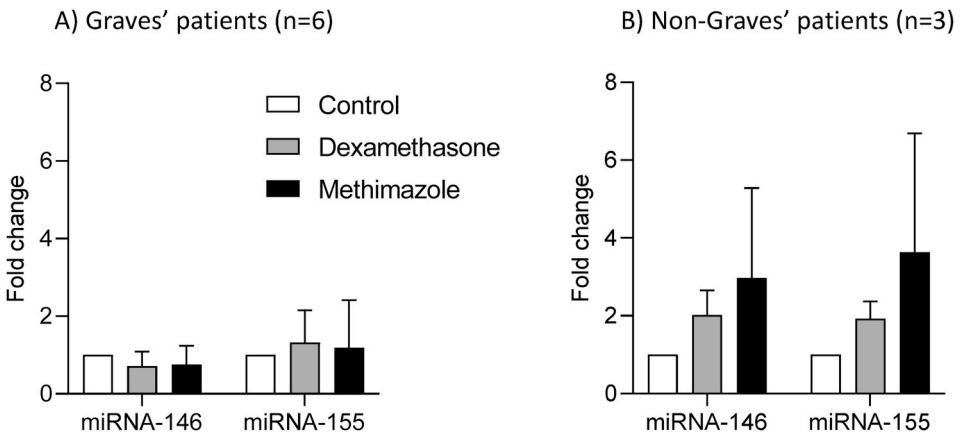

Fig. 7. qRT-PCR analysis of miRNA-146a and miRNA-155 in EV released from A) Graves' tissue (n = 6) and B) non-Graves' tissue (n = 3) maintained on a microfluidic device. Expression was normalised against miRNA-16 and fold change was calculated using $2^{-\Delta\Delta CT}$. The mean fold change from the 6 Graves' and 3 non-Graves' tissues ± SD is displayed.

the presence of viable cells at the end of the culture period. In addition Riley et al. (2019), used bromodeoxyuridine (BrdU) perfusion for the final 24 h of on-chip maintenance to demonstrate not only full thickness penetration of soluble medium constituents, but also on-chip proliferation evidenced by BrdU detection using immunohistochemistry. Further support for the retention of cell viability was demonstrated by Riley et al., through the detection of no change in apoptotic cells prior to and post microfluidic maintenance (Riley et al., 2019), as well as an array of secreted cytokines released from the same thyroid tumour tissue (Riley et al., 2021). To date the maintenance of *ex vivo* human tissue in dynamic perfusion systems has focussed mainly on the tissue itself and how time on-chip, or treatment affects the tumour architecture, protein expression and markers of viability and apoptosis, with a few looking at leakage of markers of cell death into the effluent (Hughes et al., 2021). This report however, is the first to report the use of microfluidic technology to isolate EV released from tissue maintained in a pseudo *in vivo* state. The use of microfluidic technology to isolate and characterise thyroid exosomes specific to disease pathology, utilising tissue biopsies, provides future potential to diagnose and monitor disease in a minimally invasive way using serum, urine or even tear fluid. Han et al., has observed that tear fluid exosomes are elevated in patients with thyroid eye disease compared to healthy controls and that these exosomes can induce inflammatory cytokine release from orbital fibroblasts *in vitro* (Han et al., 2021).

In the current study, EV were detectable in the microfluidic effluent throughout the six days of the experiment, following a similar pattern to the LDH release observed previously (Riley et al., 2019), with higher levels at the beginning of the experiment, again likely due to cellular disruption during experimental set-up, significantly decreasing to lower levels by day 4. It is probable that the EV in the initial effluent will consist of debris and apoptotic bodies, which is why the effluent from day 4 onwards was focussed on for the subsequent experiments. In contrast to Mobarrez et al. (2016), who found an elevated level of microvesicles in the plasma of Graves' disease patients compared to controls, using flow cytometry, and a reduction following treatment with thiamazole, no difference was observed in the levels of EV released from Graves' *vs*. non-Graves' disease tissue or with methimazole or dexamethasone treatment using NTA in the current study. However, the treatment time in the patients was months, compared to days in this *ex vivo* study and the *in vivo* drug treatment may affect EV release from other tissues. In the current study, the direct effect of dexamethasone and methimazole on exosome release were investigated, however, it should be noted that the effect of these drugs may be to influence the downstream effect of EV, which needs to be investigated further.

The nomenclature of extracellular vesicles according to the International Society for Extracellular Vesicles (ISEV), refer to vesicles with a size <200 nm as small extracellular vesicles (sEV) and those >200 nm as medium/large EV (m/lEV; Théry et al., 2018). In this context, the vesicles detected in the current study, following the initial settling down period, would be classed as sEV with only a few larger particles being released over the first few hours. Treatment did not result in a difference in the size of the vesicles released, suggesting apoptosis was not initiated during the 6 day period and although the size of the particles was consistently higher from the non-Graves tissue compared to those from Graves' tissue, this difference was not significant.

The classic exosomal markers, CD63 and CD81, were detected in a proportion of the samples investigated. However, a greater volume of tissue effluent is required to enable enhanced isolation and identification of proteins of interest in the tissue specific exosomes released during microfluidic maintenance. Exosomes from the serum of Graves' disease patients, carrying the TSH-R, IGF-1 and HSP-60 have been shown previously to induce an inflammatory response *in vitro* through the Toll-like receptor/NFκB signaling pathway, which may contribute to the pathogenesis of Graves' disease (Cui et al., 2021). The expression of IGF-1R on the exosomes released from Graves' disease tissue provides a potential mechanism for the success of treatment of Graves' disease patients with ophthalmopathy with Teprotumumab, an immunotherapy targeting this receptor (Douglas et al., 2020; Smith, 2020). These studies, emphasize the importance of further protein characterisation of disease specific exosomes from biopsy tissue.

The dysregulated expression of miRNA has been identified as playing a crucial role in the pathogenesis of several autoimmune diseases (Long et al., 2018), including Graves' disease (Martinez-Hernandez et al., 2019). A number of miRNAs have been found to be differentially expressed in the serum of patients with Graves' disease compared to those with either disease in remission (Hiratsuka et al., 2016) or healthy controls (Yao et al., 2019; Qin et al., 2015).

The current study investigated the presence of two known regulators of the inflammatory response, in exosomes released from both Graves' and non-Graves' tissue; miRNA-155 and miRNA-146a (Marques-Rocha et al., 2015). Although miRNA-146a and miRNA-155 were detectable in all tissue exosome samples, no difference in the levels expressed between the two cohorts was observed. This is in contrast to a study by Wang et al. (2017), who found a significantly elevated expression of miRNA-146a in the plasma of patients with Graves' disease (n = 27) compared to controls (n = 15). They also found that miRNA-146a directly targets *Notch 2* signaling, increasing the expression of proinflammatory IL6. However, interestingly both miRNA-146a and miRNA-155 were demonstrated to be lower in the serum of Graves' disease patients (n = 80) compared to healthy controls (n = 65) by Zheng et al. (2018). Importantly, miRNA-146a and miRNA-155 are elevated in thyroid eye disease orbital fibroblasts, whereas the expression of their targets PTEN and ZNRF3, which both inhibit proliferation, were decreased following TSH treatment of orbital fibroblasts (Woeller et al., 2019), however, as stated previously these studies are looking at whole body EV in contrast to the tissue specific EV the current study was investigating.

5. Conclusion

This proof of concept study provides a unique way to isolate tissue specific sEV/exosomes, providing the potential for rigorous screening of these EV to identify biomarkers of disease and disease severity to enable earlier identification of disease, progression monitoring throughout treatment and evidence based, personalised treatment regimens.

Ethics approval and consent to participate

The project had received ethical approval from London-Hampstead Research Ethics Committee (17/LO/0209) and was approved by Hull University Teaching Hospitals NHS trust R&D (R2469).

Funding

This work was supported by a £15, 000 grant (1 year) from the Get A-Head Charitable trust, Birmingham, UK. The funders had no role in the study design; in the collection, analysis and interpretation of data; in the writing of the report; or in the decision to submit the article for publication.

Declaration of competing interest

The authors declare that they have no known competing financial interests or personal relationships that could have appeared to influence the work reported in this paper.

Acknowledgements

The authors would like to thank the patients of Hull and East Yorkshire NHS trust who provided samples to be used in this research, the Daisy Charity for hosting the research and the Get A-Head charity for funding both the MSc studentship and consumables to carry out the

research. We would also like to thank the ENT theatre team for assisting in sample collection and Dr George Soultanidis (Translational and Molecular Imaging Institute, Icahn School of Medicine at Mount Sinai, New York) and Dr Alex Illes (University of Hull's Fabrication Facility for Lab on a Chip), for designing and making the microfluidic devices respectively.

References

Antonelli, A., Ferrari, S.M., Ragusa, F., Elia, G., Paparo, S.R., Ruffilli, I., Patrizio, A., Giusti, C., Gonnella, D., Cristaudo, A., Foddis, R., Shoenfeld, Y., Fallahi, P., 2020. Graves' disease: epidemiology, genetic and environmental risk factors and viruses, Best practice & research. Best Pract. Res. Clin. Endocrinol. Metabol. 34, 101387. https://doi.org/10.1016/j.beem.2020.101387.

Bartalena, L., Baldeschi, L., Boboridis, K., Eckstein, A., Kahaly, G.J., Marcocci, C., Perros, P., Salvi, M., Wiersinga, W.M., European Group on Graves Orbitopathy (EUGOGO), 2016. The 2016 European thyroid association/European group on graves' orbitopathy guidelines for the management of graves' orbitopathy. Eur. Thyroid J. 5, 9–26. https://doi.org/10.1159/000443828.

Bower, R., Green, V.L., Kuvshinova, E., Kuvshinov, D., Karsai, L., Crank, S.T., Stafford, N. D., Greenman, J., 2017. Maintenance of head and neck tumor on-chip: gateway to personalized treatment? Future Sci. OA. 3, FSO174. https://doi.org/10.4155/fsoa-2016-0089.

Carr, S.D., Green, V.L., Stafford, N.D., Greenman, J., 2014. Analysis of radiation-induced cell death in head and neck squamous cell carcinoma and rat liver maintained in microfluidic devices. Otolaryngol. Head Neck Surg. 150, 73–80. https://doi.org/10.1177/0194599813507427.

Catalanotto, C., Cogoni, C., Zardo, G., 2016. MicroRNA in control of gene expression: an overview of nuclear functions. Int. J. Mol. Sci. 17 https://doi.org/10.3390/ijms17101712.

Cheah, L.T., Dou, Y.H., Seymour, A.M., Dyer, C.E., Haswell, S.J., Wadhawan, J.D., Greenman, J., 2010. Microfluidic perfusion system for maintaining viable heart tissue with real-time electrochemical monitoring of reactive oxygen species. Lab Chip 10, 2720–2726. https://doi.org/10.1039/c004910g.

Cheah, R., Srivastava, R., Stafford, N.D., Beavis, A.W., Green, V., Greenman, J., 2017. Measuring the response of human head and neck squamous cell carcinoma to irradiation in a microfluidic model allowing customized therapy. Int. J. Oncol. 51, 1227–1238. https://doi.org/10.3892/ijo.2017.4118.

Contartese, D., Salamanna, F., Veronesi, F., Fini, M., 2020. Relevance of humanized three-dimensional tumor tissue models: a descriptive systematic literature review. Cell. Mol. Life Sci. 77, 3913–3944. https://doi.org/10.1007/s00018-020-03513-y.

Cui, X., Huang, M., Wang, S., Zhao, N., Huang, T., Wang, Z., Qiao, J., Wang, S., Shan, Z., Teng, W., Li, Y., 2021. Circulating exosomes from patients with graves' disease induce an inflammatory immune response. Endocrinology 162. https://doi.org/10.1210/endocr/bqaa236 bqaa236.

Dawson, A., Dyer, C., Macfie, J., Davies, J., Karsai, L., Greenman, J., Jacobsen, M., 2016. A microfluidic chip based model for the study of full thickness human intestinal tissue using dual flow. Biomicrofluidics 10, 064101. https://doi.org/10.1063/1.4964813.

Douglas, R.S., Kahaly, G.J., Patel, A., Sile, S., Thompson, E.H.Z., Perdok, R., Fleming, J. C., Fowler, B.T., Marcocci, C., Marino, M., Antonelli, A., Dailey, R., Harris, G.J., Eckstein, A., Schiffman, J., Tang, R., Nelson, C., Salvi, M., Wester, S., Sherman, J.W., Vescio, T., Holt, R.J., Smith, T.J., 2020. Teprotumumab for the treatment of active thyroid eye disease. N. Engl. J. Med. 382, 341–352. https://doi.org/10.1056/NEJMoa1910434.

Duzagac, F., Saorin, G., Memeo, L., Canzonieri, V., Rizzolio, F., 2021. Microfluidic organoids-on-a-chip: quantum leap in cancer research. Cancers 13, 737. https://doi.org/10.3390/cancers13040737.

Edo, N., Kawakami, K., Fujita, Y., Morita, K., Uno, K., Tsukamoto, K., Onose, H., Ishikawa, T., Ito, M., 2019. Exosomes expressing thyrotropin receptor attenuate autoantibody-mediated stimulation of cyclic adenosine monophosphate production. Thyroid 29, 1012–1017. https://doi.org/10.1089/thy.2018.0772.

Han, J.S., Kim, S.E., Jin, J.Q., Park, N.R., Lee, J.Y., Kim, H.L., Lee, S.B., Yang, S.W., Lim, D.J., 2021. Tear-derived exosome proteins are increased in patients with thyroid eye disease. Int. J. Mol. Sci. 22 https://doi.org/10.3390/ijms22031115.

Hattersley, S.M., Greenman, J., Haswell, S., 2011. Study of ethanol induced toxicity in liver explants using microfluidic devices. Biomed. Microdevices 13, 1005–1014. https://doi.org/10.1007/s10544-011-9570-2.

Hiratsuka, I., Yamada, H., Munetsuna, E., Hashimoto, S., Itoh, M., 2016. Circulating MicroRNAs in graves' disease in relation to clinical activity. Thyroid 26, 1431–1440. https://doi.org/10.1089/thy.2016.0062.

Hughes, D.L., Hughes, A., Soonawalla, Z., Mukherjee, S., O'Neill, E., 2021. Dynamic physiological culture of *ex vivo* human tissue: a systematic review. Cancers 13, 2870. https://doi.org/10.3390/cancers13122870.

Hurwitz, S.N., Olcese, J.M., Meckes Jr., D.G., 2019. Extraction of extracellular vesicles from whole tissue. J. Vis. Exp. https://doi.org/10.3791/59143.

Jiang, F., Chen, Q., Wang, W., Ling, Y., Yan, Y., Xia, P., 2020. Hepatocyte-derived extracellular vesicles promote endothelial inflammation and atherogenesis via microRNA-1. J. Hepatol. 72, 156–166. https://doi.org/10.1016/j.jhep.2019.09.014.

Kahaly, G.J., 2020. Management of graves thyroidal and extrathyroidal disease: an update. J. Clin. Endocrinol. Metab. 105, 3704–3720. https://doi.org/10.1210/clinem/dgaa646.

Kennedy, R., Kuvshinov, D., Sdrolia, A., Kuvshinova, E., Hilton, K., Crank, S., Beavis, A. W., Green, V., Greenman, J., 2019. A patient tumour-on-a-chip system for personalised investigation of radiotherapy based treatment regimens. Sci. Rep. 9, 6237. https://doi.org/10.1038/s41598-019-42745-2.

Kowal, E.J.K., Ter-Ovanesyan, D., Regev, A., Church, G.M., 2017. Extracellular vesicle isolation and analysis by western blotting. Methods Mol. Biol. 1660, 143–152. https://doi.org/10.1007/978-1-4939-7253-1_12.

Längericht, J., Kramer, I., Kahaly, G.J., 2020. Glucocorticoids in Graves' orbitopathy: mechanisms of action and clinical application. Ther. Adv. Endocrinol. Metab. 11 https://doi.org/10.1177/2042018820958335, 2042018820958335.

Lanyu, Z., Feilong, H., 2019. Emerging role of extracellular vesicles in lung injury and inflammation. Biomed. Pharmacother. 113, 108748. https://doi.org/10.1016/j.biopha.2019.108748.

Lee, J.C., Zhao, J.T., Gundara, J., Serpell, J., Bach, L.A., Sidhu, S., 2015. Papillary thyroid cancer-derived exosomes contain miRNA-146b and miRNA-222. J. Surg. Res. 196, 39–48. https://doi.org/10.1016/j.jss.2015.02.027.

Li, K., Du, Y., Jiang, B.L., He, J.F., 2014. Increased microRNA-155 and decreased microRNA-146a may promote ocular inflammation and proliferation in Graves' ophthalmopathy. Med. Sci. Monit. 20, 639–643. https://doi.org/10.12659/MSM.890686.

Liu, X., Qiang, W., Liu, X., Liu, L., Liu, S., Gao, A., Gao, S., Shi, B., 2015. A second course of antithyroid drug therapy for recurrent Graves' disease: an experience in endocrine practice. Eur. J. Endocrinol. 172, 321–326. https://doi.org/10.1530/EJE-14-0704.

Livak, K.J., Schmittgen, T.D., 2001. Analysis of relative gene expression data using real-time quantitative PCR and the 2(-Delta Delta C(T)) Method. Methods 25, 402–408. https://doi.org/10.1006/meth.2001.1262.

Long, H., Wang, X., Chen, Y., Wang, L., Zhao, M., Lu, Q., 2018. Dysregulation of microRNAs in autoimmune diseases: pathogenesis, biomarkers and potential therapeutic targets. Cancer Lett. 428, 90–103. https://doi.org/10.1016/j.canlet.2018.04.016.

Ma, X., Becker Buscaglia, L.E., Barker, J.R., Li, Y., 2011. MicroRNAs in NF-kappaB signaling. J. Mol. Cell Biol. 3, 159–166. https://doi.org/10.1093/jmcb/mjr007.

Mao, X.M., Li, H.Q., Li, Q., Li, D.M., Xie, X.J., Yin, G.P., Zhang, P., Xu, X.H., Wu, J.D., Chen, S.W., Wang, S.K., 2009. Prevention of relapse of graves' disease by treatment with an intrathyroid injection of dexamethasone. J. Clin. Endocrinol. Metab. 94, 4984–4991. https://doi.org/10.1210/jc.2009-1252.

Marques-Rocha, J.L., Samblas, M., Milagro, F.I., Bressan, J., Martinez, J.A., Marti, A., 2015. Noncoding RNAs, cytokines, and inflammation-related diseases. Faseb. J. 29, 3595–3611. https://doi.org/10.1096/fj.14-260323.

Martinez-Hernandez, R., Serrano-Somavilla, A., Ramos-Levi, A., Sampedro-Nunez, M., Lens-Pardo, A., Munoz De Nova, J.L., Trivino, J.C., Gonzalez, M.U., Torne, L., Casares-Arias, J., Martin-Cofreces, N.B., Sanchez-Madrid, F., Marazuela, M., 2019. Integrated miRNA and mRNA expression profiling identifies novel targets and pathological mechanisms in autoimmune thyroid diseases. E. BioMed. 50, 329–342. https://doi.org/10.1016/j.ebiom.2019.10.061.

McLean, I., Schwerdtfeger, L., Tobet, S., Henry, C., 2018. Powering *ex vivo* tissue models in microfluidic systems. Lab Chip 18, 1399–1410. https://doi.org/10.1039/c8lc00241j.

Mittal, S., Gupta, P., Chaluvally-Raghavan, P., Pradeep, S., 2020. Emerging role of extracellular vesicles in immune regulation and cancer progression. Cancers 12, 3563. https://doi.org/10.3390/cancers12123563.

Mobarrez, F., Abraham-Nordling, M., Aguilera-Gatica, K., Friberg, I., Antovic, A., Pisetsky, D.S., Jorneskog, G., Wallen, H., 2016. The expression of microvesicles in the blood of patients with Graves' disease and its relationship to treatment. Clin. Endocrinol. 84, 729–735. https://doi.org/10.1111/cen.12872.

Perez-Gonzalez, R., Gauthier, S.A., Kumar, A., Saito, M., Saito, M., Levy, E., 2017. A method for isolation of extracellular vesicles and characterization of exosomes from brain extracellular space. Methods Mol. Biol. 1545, 139–151. https://doi.org/10.1007/978-1-4939-6728-5_10.

Qin, Q., Wang, X., Yan, N., Song, R.H., Cai, T.T., Zhang, W., Guan, L.J., Muhali, F.S., Zhang, J.A., 2015. Aberrant expression of miRNA and mRNAs in lesioned tissues of Graves' disease. Cell. Physiol. Biochem. 35, 1934–1942. https://doi.org/10.1159/000374002.

Riley, A., Green, V., Cheah, R., McKenzie, G., Karsai, L., England, J., Greenman, J., 2019. A novel microfluidic device capable of maintaining functional thyroid carcinoma specimens ex vivo provides a new drug screening platform. BMC Cancer 19, 259. https://doi.org/10.1186/s12885-019-5465-z.

Riley, A.R., Jones, H., Kuvshinov, D., Green, V.L., England, J., Greenman, J., 2021. Identification of soluble tissue-derived biomarkers from human thyroid tissue explants maintained on a microfluidic device. Oncol. Lett. 22, 780. https://doi.org/10.3892/ol.2021.13041.

Smith, T.J., 2020. Teprotumumab treatment for thyroid-associated ophthalmopathy. Eur. Thyroid J. 9, 31–39. https://doi.org/10.1159/000507992.

Tanda, M.L., Piantanida, E., Liparulo, L., Veronesi, G., Lai, A., Sassi, L., Pariani, N., Gallo, D., Azzolini, C., Ferrario, M., Bartalena, L., 2013. Prevalence and natural history of Graves' orbitopathy in a large series of patients with newly diagnosed graves' hyperthyroidism seen at a single center. J. Clin. Endocrinol. Metab. 98, 1443–1449. https://doi.org/10.1210/jc.2012-3873.

Théry, C., Amigorena, S., Raposo, G., Clayton, A., 2006. Isolation and characterization of exosomes from cell culture supernatants and biological fluids. Curr. Protoc. Cell Biol. Chapter 3. https://doi.org/10.1002/0471143030.cb0322s30. Unit 3 22.

Théry, C., Witwer, K.W., Aikawa, E., Alcaraz, M.J., Anderson, J.D., Andriantsitohaina, R., et al., 2018. Minimal information for studies of extracellular vesicles 2018 (MISEV2018): a position statement of the International Society for Extracellular Vesicles and update of the MISEV2014 guidelines. J. Extracell. Vesicles 7, 1535750. https://doi.org/10.1080/20013078.2018.1535750.

Wang, N., Chen, F.E., Long, Z.W., 2017. Mechanism of MicroRNA-146a/notch2 signaling regulating IL-6 in graves ophthalmopathy. Cell. Physiol. Biochem. 41, 1285–1297. https://doi.org/10.1159/000464430.

Woeller, C.F., Roztocil, E., Hammond, C., Feldon, S.E., 2019. TSHR signaling stimulates proliferation through PI3K/akt and induction of miR-146a and miR-155 in thyroid eye disease orbital fibroblasts. Invest. Ophthalmol. Vis. Sci. 60, 4336–4345. https://doi.org/10.1167/iovs.19-27865.

Yang, D., Liu, J., 2020. Targeting extracellular vesicles-mediated hepatic inflammation as a therapeutic strategy in liver diseases. Liver Int. 40, 2064–2073. https://doi.org/10.1111/liv.14579.

Yao, Q., Wang, X., He, W., Song, Z., Wang, B., Zhang, J., Qin, Q., 2019. Circulating microRNA-144-3p and miR-762 are novel biomarkers of Graves' disease. Endocrine 65, 102–109. https://doi.org/10.1007/s12020-019-01884-2.

Yu, F., Hunziker, W., Choudhury, D., 2019. Engineering microfluidic organoid-on-a-chip platforms. Micromachines 10, 165. https://doi.org/10.3390/mi10030165.

Zhang, H.G., Liu, C., Su, K., Yu, S., Zhang, L., Zhang, S., Wang, J., Cao, X., Grizzle, W., Kimberly, R.P., 2006. A membrane form of TNF-alpha presented by exosomes delays T cell activation-induced cell death. J. Immunol. 176, 7385–7393. https://doi.org/10.4049/jimmunol.176.12.7385.

Zhang, Y., Bi, J., Huang, J., Tang, Y., Du, S., Li, P., 2020. Exosome: a review of its classification, isolation techniques, storage, diagnostic and targeted therapy applications. Int. J. Nanomed. 15, 6917–6934. https://doi.org/10.2147/IJN.S264498.

Zheng, L., Zhuang, C., Wang, X., Ming, L., 2018. Serum miR-146a, miR-155, and miR-210 as potential markers of Graves' disease. J. Clin. Lab. Anal. 32 https://doi.org/10.1002/jcla.22266.